PHYSICAL REVIEW B **66**, 075215 (2002)

Photophysics of pristine and C_{60}-doped disubstituted polyacetylene

I. I. Gontia and Z. V. Vardeny
Physics Department, University of Utah, Salt Lake City, Utah 84112

T. Masuda
Division of Polymer Chemistry, Kyoto University, Yoshida-Honmachi, Sakyoku, Kyoto 606, Japan

K. Yoshino
Department of Electronic Engineering, Osaka University, 2-1 Yamada-Oka, Suita, Osaka 565-0871, Japan

(Received 1 May 2000; published 30 August 2002)

Using a variety of steady-state spectroscopies we studied the long-lived photoexcitations and electronic excited states of poly disubstituted acetylene (PDPA-*n*Bu), the backbone structure of which is a disubstituted trans-polyacetylene, as well as PDPA-*n*Bu/C_{60} blends. The cw spectroscopies include absorption, photoluminescence (PL), photoinduced absorption (PA), and PA-detected magnetic resonance (PADMR). Although PDPA-*n*Bu is a degenerate ground-state polymer, nevertheless, and in contrast to trans-polyacetylene, we found that it has a strong PL band with quantum efficiency larger than 60%. From polarized PL studies on stretched oriented films we conclude that the PL emission originates from intrachain excitons rather than the polymer side groups. This shows that the lowest-lying exciton in PDPA-*n*Bu is a B_u state rather than an A_g state, in contrast to the order of the lowest-lying excitonic states in trans-polyacetylene. The polarized absorption in PDPA-*n*Bu contains three distinctly different bands with different polarization properties, which are interpreted according to the model of Shukla and Mazumdar. The PA spectra of pristine and photo-oxidized PDPA-*n*Bu films show neutral and charged solitons as well as polaron excitations, whereas the long-lived photoexcitations in PDPA-*n*Bu in solution are mainly polarons. This may be due to destabilization of the soliton-antisoliton pairs in the polymer chains in solution caused by short conjugation length. From the PA and PADMR spectroscopies of PDPA-*n*Bu/C_{60} blends we conclude that a photoinduced charge-transfer reaction takes place, again in contrast to blends of other nonluminescent polymers. Interestingly the PA spectrum of PDPA-*n*Bu/C_{60} blends shows both charged polarons and charged solitons that are correlated with the PA band of C_{60}^-. We found that the ratio between charged solitons and polaron excitations depends on the C_{60} concentration in the blend, the film morphology, and temperature. It is shown that the mechanism by which two polarons on the same PDPA-*n*Bu chain recombine into two charged solitons is the dominant process that determines the soliton/polaron ratio in the blends.

DOI: 10.1103/PhysRevB.66.075215 PACS number(s): 71.38.−k, 71.55.Ht, 76.70.Hb, 78.40.Me

I. INTRODUCTION

It has been shown that the emissive and nonlinear optical properties of the centrosymmetric π-conjugated polymers are determined by the order of the two lowest excited states[1–3] with odd and even symmetry, namely, $1B_u$ and $2A_g$, which are determined by electron correlation and the size of the bond alternation (g stands for even parity and u for odd parity). For the C_{2h} symmetry group electrical dipole transitions are allowed between states with opposite parity. It has been established that in nonluminescent polymers the $2A_g$ level is lower than $1B_u$, whereas in luminesent polymers the $2A_g$ state is higher than the $1B_u$ state.[3]

The disubstituted polyacetylene, PDPA-*n*Bu (displayed in Fig. 1) is similar to trans-polyacetylene, where one side group is a phenyl ring and the other is a phenyl attached to a butyl group,[4] Although PDPA-*n*Bu is a degenerate ground-state (DGS) polymer as was deduced from doping experiments,[5] nevertheless it has strong photoluminescence (PL), which conflicts with what is known about the DGS polymers.[6] Unlike the other luminescent π-conjugated polymers, where the order of the lowest-lying excitons has been explained as a result of the large dimerization,[3] in PDPA-*n*Bu the order $1B_u$-$2A_g$ was attributed to the small electron-electron interaction.[7,8]

The polarized absorption spectra of PDPA-*n*Bu were recently calculated,[7] revealing the existence of three absorption bands: (i) a lower-energy band associated with intrachain exciton transitions, (ii) an intermediate-energy band that originates from transitions between the chain backbone states

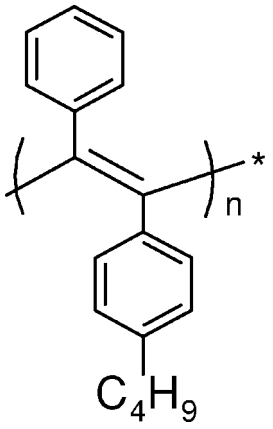

FIG. 1. The backbone structure of PDPA-*n*Bu.

and states of the phenyl rings [charge-transfer (CT) exciton transitions], and (iii) a strong band in the high-energy range (≈6 eV) that is due to the phenyl side groups.

Picosecond transient photoinduced absorption (PA) measurements were completed in PDPA-*n*Bu films at low excitation intensity, and it was found that an exponential decay with lifetime τ=600 ps fits the data well.[5] The radiative lifetime τ_r was calculated using the relationship for the PL quantum efficiency $\eta = b\tau_r/\tau$, where b was the photogeneration efficiency of the relaxed exciton $(1B_u)_r$, which was assumed to be 1. For η=50% the radiative lifetime was calculated to be τ_r=1.2 ns. This is close to the radiative lifetime of PPV that is known as a strong luminescent π-conjugated polymer.[9]

The time-resolved PL in PDPA-*n*Bu film was also investigated.[10] It was shown that there is a spectral dependence of the PL decay time, displaying a double exponential decay at shorter emission wavelength (for 475 nm τ_1 =0.10 ns and τ_2=1.2 ns) and a single exponential decay at longer emmission wavelengths (for λ=625 nm, τ=2.74 ns). This shows that the PL component with shorter wavelength is faster than that with longer wavelength, indicating exciton migration to longer chains with lower excitation energy. The lack of overlap between PL and absorption and its high quantum efficiency make PDPA-*n*Bu suitable for optical applications such as laser action[11] and light emitting diodes (LED).[12] It was found that in PDPA-*n*Bu films there is high optical gain when excited with short optical pulses at moderately high excitation intensities. Above a threshold excitation level of about 1 MW/cm^2, which is considered to be relatively low, it was found[11] that the emission bandwidth around 510 nm narrows from 100 nm to below 10 nm.

CT processes in π-conjugated polymer/C_{60} blends have been investigated in a series of studies.[13–17] In some polymer/C_{60} mixtures the CT process from the polymer to C_{60} takes place in the ground state,[18] whereas in many others it is photoinduced.[13–17] The photoinduced CT between the π-conjugated polymer chains and the C_{60} molecule is governed by energetics, i.e., by the relative position of the polymer energy levels with respect to those of the C_{60} dopant.[19] The quenching of PL, the increase of the photocurrent, and the absorption band of C_{60}^- in the PA spectrum have provided evidence for photoinduced CT in C_{60} doped polymers.[13–17] Transient spectroscopy measurements have demonstrated that the forward CT process is very fast, occurring in less than 10^{-12} s following the pulse excitation.[20] The studies of weak infrared PL, which results from radiative electron-hole recombination between the fullerene excited state and polymer ground-state revealed that the backward process is very slow.[21] This is due to the large size of the C_{60} dopant molecules that stabilizes the charge separation. The electron added to the spherical C_{60} molecule is self-trapped, forming a polaron with a charge distributed mostly along the equatorial line of the molecule and a lattice distortion with a minimum dimerization along the same line.[22]

Studies of photoinduced electron transfer focusing on the effect of strong Coulomb correlation have shown that the strong Coulomb binding of the electron and hole in the excited states inhibits the photoinduced electron transfer from polydiacetylene onto C_{60}.[23] It was concluded that in luminescent polymers, such as poly(3-alkylthiophene) [P3AT] and poly(*p*-phenylene vinylene) [PPV] where the photoinduced CT reaction was observed, the Coulomb interaction is sufficiently well screened so that upon photoexcitation the photoinduced CT reaction can take place. In the theoretical model elaborated for CT in a molecularly doped conjugated polymer presented in Ref. 24, it was shown that the photoinduced CT due to exciton dissociation between a polymer chain and an acceptor molecule reaches a maximum when Δ, the energy difference between the dopant-polymer HOMO levels, is approximately equal to the exciton binding energy.

The paper presents CW spectroscopic studies of pristine PDPA in films and solutions and blended with C_{60}. In Sec. II we present the experimental techniques used in our measurements. Section III presents the absorption and PL spectroscopic results of PDPA-*n*Bu in the form of stretched oriented films, as well as long-lived photoexcitations in pristine films and in toluene solution using PA and PA-detected magnetic resonance (PADMR) techniques. We also show evidence of photoinduced CT in films of PDPA-*n*Bu/C_{60} blends. Section IV summarizes the results.

II. EXPERIMENTAL METHODS

PDPA-*n*Bu powder was synthesized using diphenylacetylene monomers and the $TaCl_5$-Bu_4Sn catalyst.[25,26] Thin films of pristine PDPA-*n*Bu were prepared from toluene by spin casting or dropcasting on KBr or sapphire substrates. The solution of the PDPA-*n*Bu/C_{60} mixture was prepared by mixing C_{60} in xylene with PDPA-*n*Bu dissolved in xylene of appropriate ratio to get the desired C_{60}/PDPA-*n*Bu weight ratio. The photo-oxidized samples were prepared by exposing the polymer films to laser light in air.[27] To obtain stretched films, the polymer solution was dropcasted onto a polyethylene substrate and manually stretched to achieve various stretching ratios.[28]

The PA technique has been extensively used in semiconductors for the detection of a long-lived photogenerated species sample by measuring the change, ΔT in transmission, T of the probe light due to the absorption of the photogenerated species.[29] The spectral response of the optical setup is eliminated when dividing ΔT by T. ΔT is corrected for the PL of the sample. Therefore, the quantity that is measured is

$$\frac{\Delta T}{T} = \frac{T_{on} - T_{off} - PL}{T_{off}}, \tag{1}$$

where T_{on} (T_{off}) is the transmission through the sample with the laser light on (off).

The PA spectra were obtained at 80 K using an Ar^+ laser (Coherent, Inova 90 series) beam at 458 nm or 360 nm. The laser beam was modulated with a mechanical chopper (Stanford Research Systems, Inc, Model SR540) at a typical frequency of 100 Hz. The probe beam was derived from a tungsten-halogen lamp (Osram HLX 64655) in the spectral range 500 nm–2.4 μm, and a glow bar for the range 2.4–15 μm. A parabolic mirror directed the transmitted light through the sample onto the entrance slit of a (1/4)-meter monochromator (Aries, Model MC 20). At the exit slit of the mono-

chromator the light was detected by a solid-state photodetector. Depending on the spectral range, the following detectors were used: Si(UDT Model 10DP/SB or UV100), Ge(EG&G Judson Model JD-16), InSb (EG&G Judson Model JD-14), and MCT (EG&G Judson Model JD). The signal from the detector was preamplified and detected by means of a lock-in amplifier (EG&G Princeton Applied Research Model 5209, Stanford Research Systems Model SR 830 DSP) referenced to the pump beam modulation. Several long pass filter and grating combinations were used to cover the entire spectral range of our measurements, which was 0.1–2.5 eV. The PL spectrum was measured with the same setup except that the probe light was blocked. The PL spectrum was also corrected for the spectral response of the apparatus.

To obtain the midinfrared region of the PA spectrum, a PA setup based on a Fourier transform infrared (FTIR) spectrometer was also used.[30,31] The FTIR spectrometer was modified such as to allow access for a cryostat and laser beam. A shutter was used to turn the laser illumination on the sample on and off. The PA spectrum was obtained by taking a number of scans with the laser on and the same number of scans with the laser off, opening or closing the shutter. A large number of scans were recorded to get a good signal-to-noise ratio and overcome the detection limitation established by the digitization resolution.[31] The total number of scans is the product between the number of the scans chosen for one sweep, which gives the average spectrum, with the laser on (off), and the number of sweeps with the laser on (off). The measurements were run by a macro based on OPUS commands, which performed a number of loops to produce the data files of the spectra with the laser on and off, respectively.[30]

The PADMR setup contains, in addition to the regular PA setup, the electron magnetic-resonance part.[29] It consists of a high-Q magnetic-resonance cavity with windows for the optical transmission, a magnet to generate a dc magnetic field, a microwave generator, and a microwave modulator. The microwaves were introduced into the resonant cavity through a waveguide. The sample was placed in a cryostat and cooled to liquid-He temperature. The changes, δT in transmission, T of the probe light through the sample in the dc magnetic field with the excitation laser on, due to the microwave absorption, were measured using a phase-sensitive technique. Two types of PADMR spectra were measured:[32] the λ-PADMR spectrum in which the wavelength is scanned keeping constant the dc magnetic field at resonance, and the H-PADMR spectrum where the magnetic field is scanned keeping constant the probe wavelength. The custom-made microwave cavity was a 3-GHz coaxial resonant cavity operating in a TEM_1 mode. The microwaves were generated by a Hewlett-Packard (HP) Model 616 A uhf generator, which produces signals of frequencies in the range 2–4 GHz. The microwaves were modulated with an HP 11720A pulse modulator and amplified by a rf amplifier (Mini-Circuit, Model ZHL-5) with a maximum output power of 1 W that was introduced into the waveguide connected to the cavity.[33] A function generator (BK precision 3010) provided the reference signal for the lock-in amplifier and the signal for the input modulator. The modulation frequency was set between 100–200 Hz.

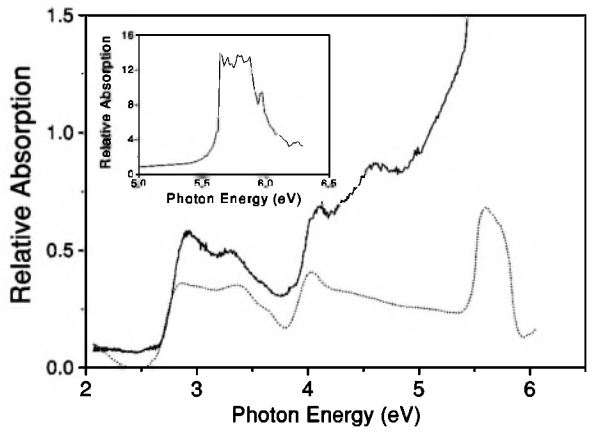

FIG. 2. The absorption spectra of PDPA-nBu films: unstretched (solid line) and stretched oriented (dotted line). The inset shows the absorption spectrum of an unstretched film above 5 eV.

The superconducting magnet (American Magnetics, Inc. product) generated a dc magnetic field in the range 0–30 000 G, with homogeneity of $\pm 1 \times 10^{-4}$ G. The current through the superconducting magnet was controlled by the computer through a digital-to-analog converter with a minimum magnetic field step of 1 G. The magnet was kept at liquid-He temperature. The $\delta T/T$ overall sensitivity of the apparatus was of the order of 10^{-8} (Ref. 33).

III. RESULTS AND DISSCUSION

A. Undoped PDPA-nBu

1. Absorption spectroscopy

Figure 2 shows the optical-absorption spectrum of a drop-cast PDPA-nBu film on polyethylene substrate. The absorption spectrum was corrected for the absorption of the substrate. The sharp rise at the absorption onset implies a narrow distribution of the polymer conjugation length. The absorption spectrum exhibits three distinct spectral features. The broad, low-energy band with its vibronic progression peaking at 2.93 eV and 3.29 eV, respectively, is assigned to the absorption of the π-π^* intrachain exciton. The middle part of the spectrum with peaks at 4.13 eV and 4.64 eV, respectively, is assigned to the absorption of a CT exciton due to transitions between the backbone polymer chain and the benzene side groups.[7] The strong high-energy band peaking at 5.75 eV corresponds to the absorption of the benzene molecule, and is displayed more clearly in the inset of Fig. 2.

The absorption spectra with polarization parallel (x) and perpendicular (y) to the drawing axis of the stretched film of PDPA-nBu are displayed in Figs. 3(a) and 3(b), respectively.[5] The stretched oriented film was obtained by stretching the polyethylene stripe to a 5.6:1 ratio. As a reference for the absorption spectra we used a polyethylene sheet that was stretched at the same ratio as the sample, and measurements were done with an identical polarizer with that placed in the sample channel. The absorption spectrum with incident light polarized parallel to the drawing axis x shows only two distinct features: the low-energy π–π^* band with the peak of the 0–0 transition at 2.90 eV and a featureless

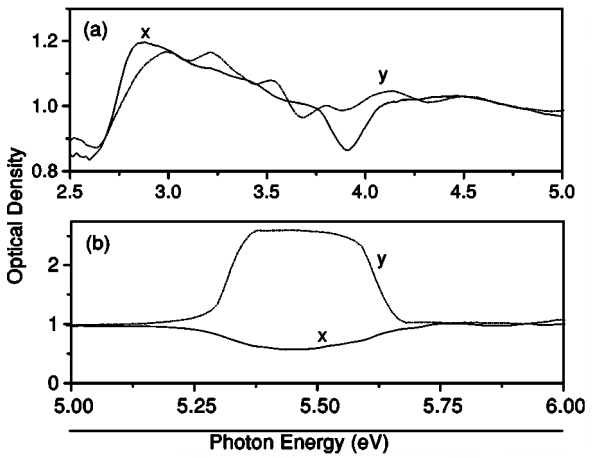

FIG. 3. The polarized absorption spectra of a stretched oriented PDPA-nBu film: (a) x-polarized (solid line) and y-polarized (dash-dotted line) absorptions between 2 to 5 eV, (b) x-polarized (solid line) and y-polarized (dash-dotted line) absorptions above 5 eV.

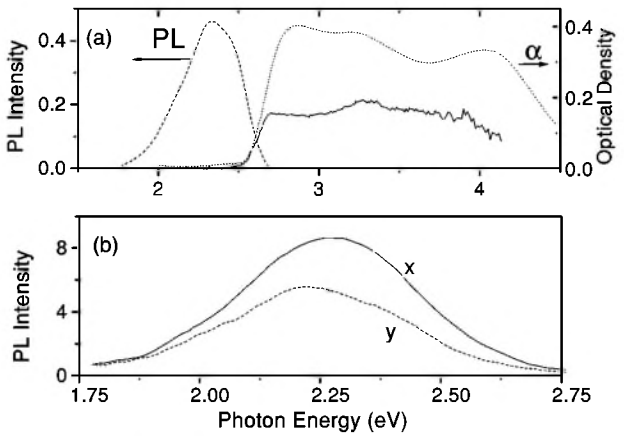

FIG. 4. (a) PL (dashed line), absorption (solid line), and PL excitation (dashed line) spectra of PDPA-nBu, (b) x-polarized (solid line) and y-polarized PL band (dotted line) of a stretched oriented PDPA-nBu film.

broadband extended between 4 eV and 4.8 eV, assigned to CT transitions. The high-energy band that is ascribed to the benzene moiety, which is very strong in the unstretched sample, is however absent in the parallel polarized absorption spectrum. The absorption band with polarization perpendicular to the drawing direction shows a blueshift in the low-energy band, with the 0–0 peak transition (y) at 3 eV and a well-defined vibronic structure associated with it, implying a simple vibronic activity with a narrow distribution of the phonon energy. Stretching does not to affect much the perpendicular absorption component.

The CT-type absorption features are associated with absorption bands at 4.13 eV and 4.55 eV, respectively. The 4.13-eV band is the same location as that in the absorption of the unstretched sample indicating that stretching does not affect this transition. The assignment of this band as CT-type absorption is thus consistent with its small dependence on polarization. The strong band at 5.42 eV due to the absorption of the benzene moiety is ascribed to transitions among localized orbitals, l–l^*, which according to the theoretical prediction should be y polarized.[7,28]

2. Photoluminescence spectroscopy

Figure 4(a) shows the absorption, PL, and PL excitation spectra of a PDPA-nBu film. The PDPA-nBu film has strong PL with quantum efficiency higher than 60%, as measured with an integrated sphere. The PL spectrum consists of a broadband peaked at 2.4 eV with no vibronic structure. It exhibits a relative large Stokes shift between the first absorption peak and the PL peak.[34]

The PL excitation spectrum shows that there is a small excitation band below the gap, followed by a sharp rise at the absorption onset. This result is consistent with a narrow distribution of the polymer conjugation length; most of the PL originates from intrachain excitons that are created on chains with a short conjugation length, which then migrate to longer chains where radiative recombination takes place.[10] The approximate step-function shape of the excitation spectrum indicates that the emission directly follows the relaxation process.[35] The peak in the excitation spectrum at 3.29 eV at the first vibrational level of the $1B_u$ is associated with the fast radiative recombination component that takes place in the same chain where the exciton was initially photogenerated. The PL emission that originates from the other excited states takes place after thermalization is completed, as the result of the exciton migration to chains with larger conjugation length, and is associated with the slow component of the transient PL decay.[10]

The PL of the stretched oriented film measured by rotating the analyzer in front of the monochromator, displayed in Fig. 4(b), shows a PL polarization anisotropy with preference along the stretching direction. This proves that the emission comes from the polymer chain rather than the side groups.[34]

3. Photoinduced absorption spectroscopy

Figure 5 exhibits the PA spectra of (a) a pristine PDPA-nBu film, (b) an oxidized PDPA-nBu film, and (c) pristine PDPA-nBu in toluene solution. Pristine PDPA-nBu films [Fig. 5(a)] show mainly a single PA band at 1.7 eV, which is due to neutral photoexcitations that are associated with spin 1/2, and therefore this PA was identified as due to photogenerated neutral soliton-antisoliton pairs (S^0-$\bar{S}^0$).[5] These species are probably photogenerated in the picosecond time domain, together with intrachain excitons.[36] The branching ratio between the neutral soliton pairs and intrachain excitons is not known at the present time. Several mechanisms have been advanced[5] to explain the process by which the neutral soliton pairs are photogenerated in PDPA polymers. One mechanism may be the dissociation of the $2A_g$ state into two soliton-antisoliton pairs during the hot exciton thermalization process following photon absorption.[37,38] Another mechanism may be a triplet exciton dissociation into a soliton-antisoliton pair following intersystem crossing from the singlet to the triplet manifold.[39] The question of which mechanism is viable in PDPA-nBu may be resolved by picosecond pump-probe measurements, which actually are underway in our laboratory at the present time.[36]

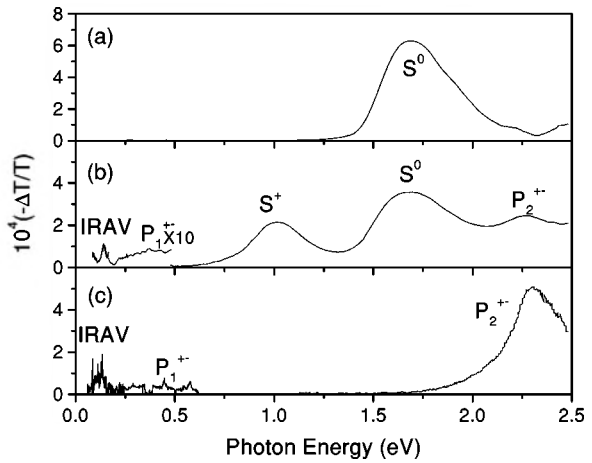

FIG. 5. The PA spectra of (a) pristine PDPA-nBu in toluene solution, (b) pristine PDPA-nBu film, and (c) photo-oxidized PDPA-nBu film. The polaron (P_1,P_2), neutral soliton (S^0), and charge soliton ($S^{\pm}$) absorption bands are assigned; IRAV stands for infrared active vibrations.

The PA spectrum of photo-oxidized PDPA-nBu [Fig. 5(b)] contains, in addition to the S_0 PA band at 1.7 eV, also three other bands at 0.3, 1.0, and 2.5 eV, respectively.[5,27] These PA bands are correlated with a strong photoinduced infrared active vibration (IRAV) band at 0.16 eV indicating that they are due to charged species.[40] The strong PA band at 1.0 eV is similar to a doping induced absorption band in PDPA and therefore was identified[5] as due to charged solitons (S^+ and S^-). The two other bands at 0.3 and 2.5 eV, respectively, were shown to correlate to each other, and be associated with spin 1/2, and therefore were identified[27] as due to photogenerated polarons. It is worth noting that PDPA-nBu is the first DGS polymer in which both long-lived charged polarons and solitons are simultaneously present in the PA spectrum.[6]

The PA spectrum of PDPA-nBu in toluene solution [Fig. 5(c)] shows only two PA bands at 0.3 and 2.5 eV, respectively. The similarity of these PA bands to those of the photo-oxidized film [Fig. 5(b)] is obvious and thus, similarly as for the photo-oxidized film, we also identify the PA bands in PDPA-nBu in solution as due to polaron excitations. We conjecture that there exists a photoinduced CT reaction between the polymer chain and solvent molecule, in which the photogenerated exciton on the polymer chain dissociates into an anion on the solvent molecule and a positive polaron on the polymer chain.[41] This mechanism is similar to the well-known photoinduced CT process that occurs in polymers doped with C_{60}.[13,14]

Intrinsic processes that lead to polaron formation in PDPA-nBu in solution could also exist. One possible process is electron hopping between chains stacked on to each other in a bunch, where the interchain distance is small. Another process is electron hopping on the same chain among different conjugated segments separated by torsion points that interrupt the chain conjugation, or on different chains bonded by crosslinks. The cw PA results in solution are supported by the PA transient results presented in Ref. 42, where polaron photogeneration was reported. The time-resolved PA spectra between 1.7 eV and 2.95 eV, measured at different delay times showed that a long-lived PA feature at 2.3 eV starts emerging after 200 ps and persists for hundreds of nanoseconds. The broadband at 0.23 eV that contains the IRAV features was measured to have the same dynamics as that of the high-energy PA band at 2.3 eV. The time-resolved PA spectrum for time below 200 ps displays a PA band at 1.7 eV, which was assigned to excitons.[42] Thus some of the excitons in PDPA-nBu in toluene solution dissociate into polarons in about 200 ps.

From the PA spectrum in PDPA-nBu in solution, in contrast to PDPA-nBu films, we do not observe long-lived neutral and charged solitons. Since the CT reaction between the polymer chain and the solvent molecule is relatively slow (200 ps),[42] this permits the generation of long-lived neutral solitons in the polymer chains either via $2A_g$ (Refs. 37 and 38) or via triplet dissociation[39] following intersystem crossing. Also two adjacent polarons on the same chain would eventually recombine to form long-lived charged solitons.[6] To explain these seemingly contradictory facts we therefore conclude that soliton excitations are unstable on the polymer chains in solution. This may be related to the small polymer conjugation length in solution, which is in agreement with the PDPA-nBu absorption blueshift that was observed in solution.[30] Since solitons are topological excitations and therefore are created in pairs of solitons and antisolitons, then the polymer chains simply do not contain long enough conjugations to permit two topological phase changes that characterize soliton-antisoliton[6] pair excitations. Resonant Raman-scattering studies in films of PDPA-nBu have indicated[34] that the mean chain conjugation is short, of about seven repeat units. In solution the bulky side groups may more easily rotate and thus further shorten the mean conjugation to be below about five repeat units. This short conjugation would destabilize topological soliton excitations because of the excess energy associated with two-phase changes associated with a soliton-antisoliton pair.

B. C_{60} doped PDPA-nBu

1. PA spectroscopy

The energy diagrams of the PDPA-nBu polymer and C_{60} molecule are shown in Fig. 6. Having its LUMO level within the gap of the polymer, C_{60} is thus a weak dopant for PDPA-nBu. Therefore a CT process is expected to occur in the excited state, either by exciting the polymer chain or the dopant C_{60} molecule.

The visible near IR absorption spectra of pristine PDPA-nBu and C_{60} doped PDPA-nBu are shown in Fig. 7(a) and compared with the absorption spectrum of I_2-doped PDPA-nBu. The steep onset of the absorption spectrum of pristine PDPA-nBu suggests a relatively defect-free film with a narrow conjugation length distribution. In the PDPA-nBu/C_{60} blend the weak absorption of C_{60} caused by an allowed dipole transition at 3.7 eV is also observed. The absorption tail below the gap in the blend is associated with an increase in the width of the conjugation length distribution and also with weak absorption of the C_{60} molecule due to a dipole forbidden transition at 1.8 eV highest occupied

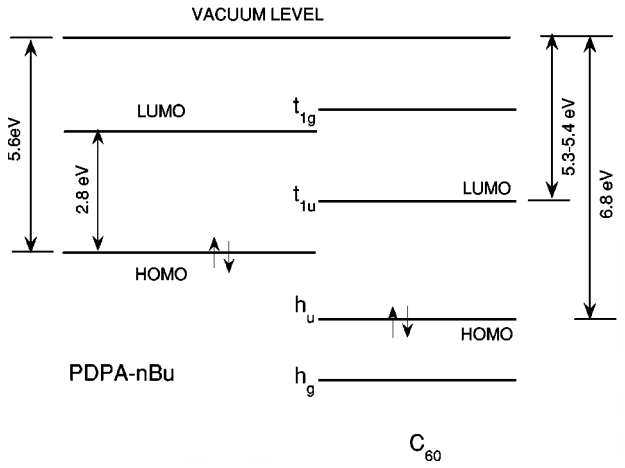

FIG. 6. The energy-level diagram of PDPA-nBu and C_{60} molecule.

molecular orbital [(HOMO): h_u] to lowest unoccupied molecular orbital [(LUMO): t_u]; these usually become partially allowed after doping probably as a result of the symmetry breaking.[43]

The absorption spectrum of the PDPA-nBu/C_{60} blend in the midinfrared range [Fig. 7(b)] shows that there is no new IRAV feature, indicating that electron transfer from the polymer chain to C_{60} molecule does not take place in the ground-state. If CT would have taken place, then an absorption band around 1250 cm^{-1} would be seen, as in the absorption spectrum of iodine-doped PDPA-nBu (Ref. 5) [also shown in Fig. 7(b)].

Figures 8(a)–8(c) illustrate the PA spectra of PDPA-nBu/C_{60} films of different C_{60} concentrations: 0.5%, 3%, and 7%, respectively. The PA spectra were measured at 80 K using the 2.73-eV Ar^+ laser line with a power of 250 mW. The spectra show the characteristics of PA bands of both charged (S^+) and neutral (S^0) solitons, and, in addition, two PA bands at 0.37 eV and 2.35 eV, respectively, which we assigned to P_1 and P_2 transitions of polarons (P^+), similar

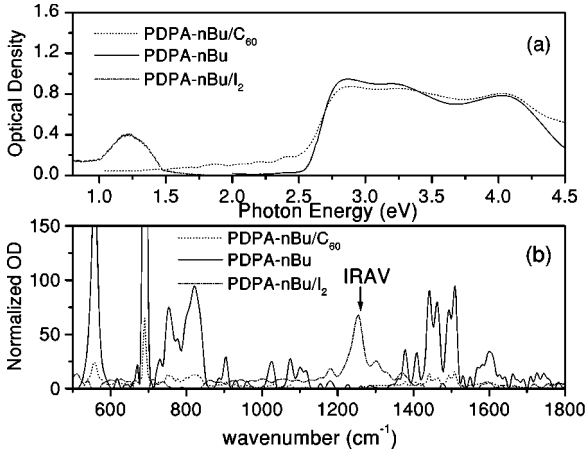

FIG. 7. The absorption spectra of I_2-doped and undoped PDPA-nBu compared with the absorption spectrum of PDPA-nBu/C_{60} mixture in (a) visible spectral range and (b) infrared spectral range.

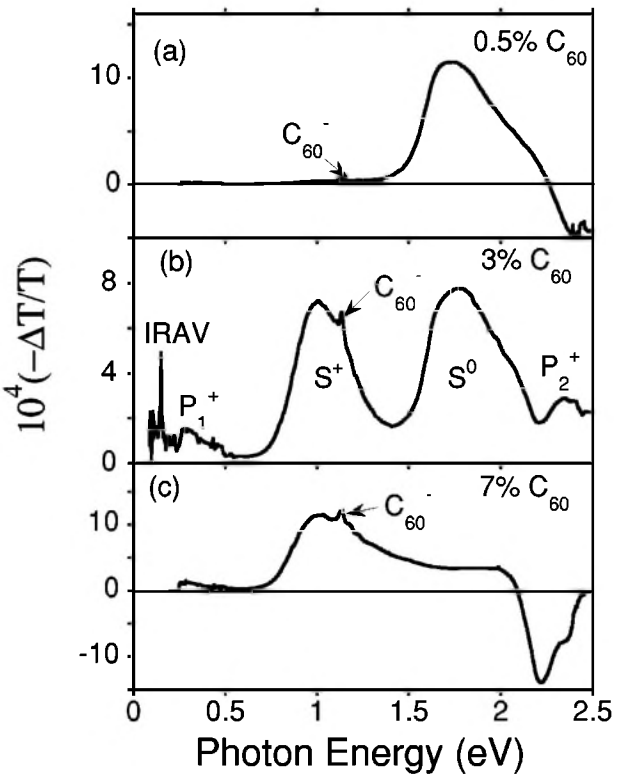

FIG. 8. The PA spectra of PDPA-nBu/C_{60} mixtures at different C_{60} concentrations: (a) 0.5%, (b) 3%, and (c) 7%. The P_1, P_2, S^+, S^0, C_{60}^-, EA absorption bands are assigned.

as in pristine PDPA-nBu (see Sec. III A 3). It is seen that the polaron bands diminish at higher C_{60} concentration as discussed in Ref. 27. The photoinduced infrared active vibrations (IRAV) are the signatures of photogenerated charged excitations on the polymer chains.[44] Its huge oscillator strength is caused by the small kinetic mass of the species.[40] In PDPA-nBu/C_{60} mixtures we also observe a clear signature of a photoinduced CT process; namely, a sharp PA band at 1.15 eV that is due to photogenerated C_{60}^-;[16] this occurs as a result of photoinduced electron transfer from the polymer chain onto the C_{60} molecule. It has been shown that C_{60} itself does not have any absorption features or PA bands between 0.05 and 1.4 eV;[17] the peak at 1.15 eV and its vibronic structures are therefore due to C_{60}^-. These transitions were also observed in the absorption spectrum of C_{60} that was induced and generated by γ-ray irradiation.[45]

The PA spectra of the PDPA-nBu/C_{60} mixture for the 7% C_{60} concentration that was obtained with UV laser excitation (see Fig. 9) exhibit approximately the same features as those excited with the visible laser light. The slight modification is the appearence of the PA band due to the C_{60} triplet-triplet transition at 1.7 eV (Ref. 46) that is superimposed on the S^0 PA band. The photobleaching (PB) below the band gap is due to C_{60} electroabsorption (EA) that overlaps with the PA of the blend spectrum; it may be due to the electric field induced by the photogenerated carriers.[47] As was shown in Ref. 48, C_{60} exhibits EA spectral features around this spectral range. The CT process is sample dependent due to C_{60} segregation in the parent solution.[30] Comparing the PA spectrum of photo-oxidized PDPA-nBu film with that of the

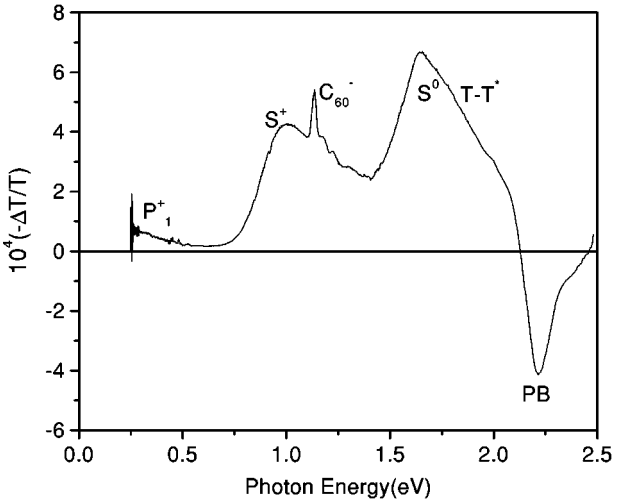

FIG. 9. The PA spectrum of PDPA-*n*Bu doped with 7% C_{60} measured with UV excitation.

PDPA-*n*Bu/C_{60} composite, we conclude that C_{60} molecules in the polymer/C_{60} blend play the same role as the defects sites in the photo-oxidized PDAP-*n*Bu film.[27]

To find the nature of the different PA bands in the PDPA/C_{60} blend we investigated the PA dependencies on laser power and frequency.[35,49] In Fig. 10(a) we show the chopper frequency dependence of the various PA bands measured at a laser power of 100 mW. The lifetime of the photogenerated carriers was determined by fitting the experimental data with a monomolecular recombination process assuming a rectangular lifetime distribution, this model was presented in Ref. 47. For the photogenerated polarons we got a decay time distribution between 0–6 ms, for the charged solitons between 0–3 ms, and for the neutral solitons between 0–6 ms.

The laser intensity dependencies of the 0.37-, 1.2-, and 1.7-eV PA bands are displayed in Fig. 10(b). The neutral soliton peak obeys a power law of $I^{0.89}$ reafirming its mono-

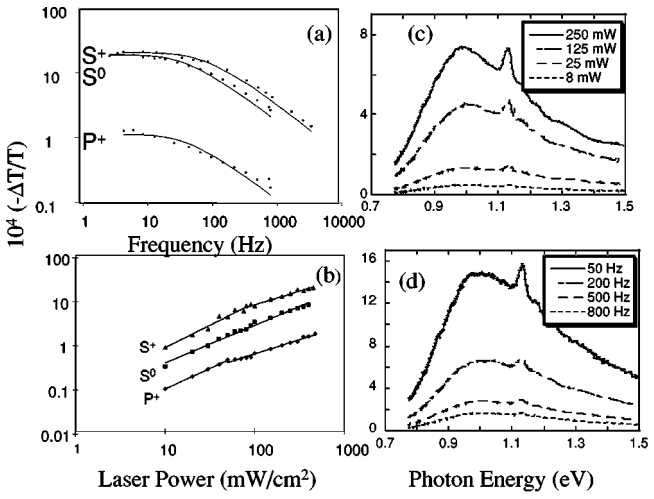

FIG. 10. The dependence of the different PA bands in 7% PDPA-*n*Bu/C_{60} film on (a) chopper frequency, (b) pump intensity. The dependence of the S^+ and C_{60}^- PA bands on (c) the pump intensity and (d) the chopper frequency.

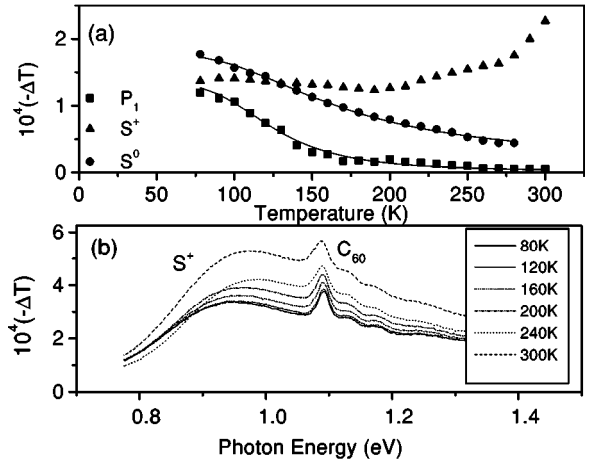

FIG. 11. The temperature dependence of the PA bands in 7% PDPA-*n*Bu/C_{60} blend for (a) polarons (squares), charged solitons (triangles), and neutral solitons (circles), and (b) the charged soliton and C_{60}^- bands.

molecular recombination kinetics. A different dependence is exhibited by the positive charged soliton S^+ and polaron P^+ bands. S^+, the PA signal, increases approximately as $I^{1.02}$ for laser intensity up to 100 mW, and as $I^{0.62}$ at higher laser power. This means that a monomolecular recombination kinetics is present at low laser intensity, whereas a bimolecular kinetics[50] becomes dominant at higher laser excitation intensity.[49,50] The polaron band also shows a $I^{0.99}$ power law, meaning a monomolecular recombination kinetics behavior up to 80 mW and bimolecular behavior above it, with a power law of $I^{0.64}$. The similar intensity and frequency dependencies of S^+ and C_{60}^- PA bands given in Figs. 10(c) and 10(d) show that the process by which S^+ and C_{60}^- are photogenerated is correlated.

The temperature dependence of the three dominant PA bands in PDPA-*n*Bu/C_{60} is exhibited in Fig. 11(a). They show different temperature dependencies. The soliton and polaron PA dependence on the temperature were fitted with a model presented in Ref. 51. The model allows to obtain the energy levels and the concentration of the dominant traps.

We note that the charged soliton PA signal remains constant up to 140 K, decreases slightly up to 200 K, and then monotonical increases above 200 K. The local minimum of the soliton PA signal at 200 K coincides with a small increase in the population of polarons. The evolution of the S^+ and C_{60}^- PA with temperature [Fig. 11(b)] indicates that the absorption of the C_{60}^- PA band does not change when the temperature increases. It stays the same on top of the S^+ band, which however increases with the temperature. This implies that there is a process that depends on the temperature, which creates S^+ from polarons but without involving the C_{60} molecules. This can be explained using the following scenario: The photoinduced polarons are stabilized by the C_{60}^- anions and this reduces their mobility. When the temperature increases then the polaron mobility also increases, favoring the encounter between two polarons on the same chain, as well as a neutral soliton encounter with a polaron. Thus, the reac-

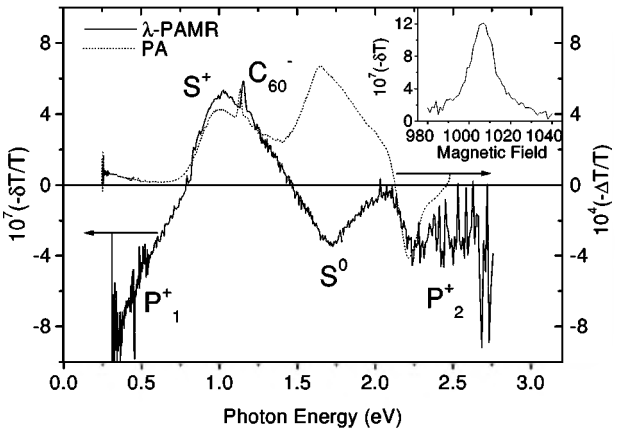

FIG. 12. The PA spectrum of 7% PDPA-nBu/C_{60} mixture (dotted line) compared with the λ-PADMR spectrum at $H=1010$ G (solid line) for $s=1/2$ resonance. The inset is the H-PADMR at 2900 nm.

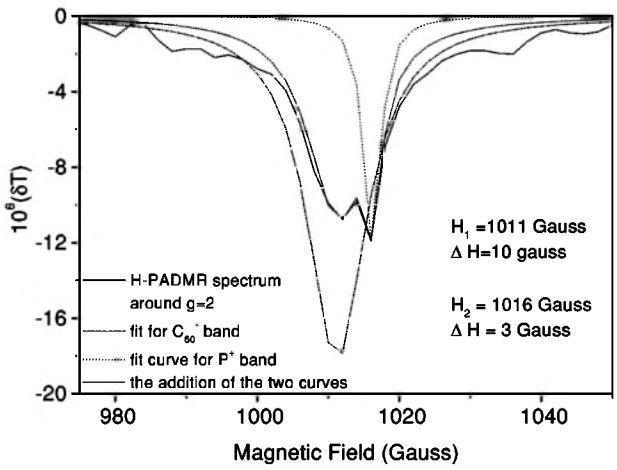

FIG. 13. The H-PADMR spectrum at 1090 nm showing two resonances at H_1 and H_2 due to polarons and C_{60}^-, respectively. The fit to the data using two different Lorentzians is also shown.

tions leading to the charged soliton population enhancement at high temperature are

$$P^{\pm}+P^{\pm}\rightarrow S^{\pm}+\bar{S}^{\pm}, \tag{2}$$

$$S^0+P^{\pm}\rightarrow S^{\pm}. \tag{3}$$

At low temperatures the polaron and charged soliton generation is mainly an extrinsic process mediated by the C_{60} dopant. A polaron is generated via exciton dissociation on an adjacent C_{60} molecule

$$\mathrm{Ex}+\mathrm{C}_{60}\rightarrow P^{+}+\mathrm{C}_{60}^{-}, \tag{4}$$

whereas the charged solitons are generated when two excitons dissociate into two adjacent C_{60} molecules close to one another on the same polymer chain,

$$2\mathrm{Ex}+2\mathrm{C}_{60}\rightarrow P^{+}+P^{+}+2\mathrm{C}_{60}^{-}\rightarrow S^{+}+\bar{S}^{+}+2\mathrm{C}_{60}^{-}. \tag{5}$$

The polarons may be also created via C_{60} exciation, when a hole transfer takes place from the C_{60} to the the polymer chain upon C_{60} photoexcitation. Indeed the polaron action spectrum shows a sharp increase above 3.5 eV,[27] which may be correlated with the excitation of the C_{60} molecule.[43]

2. PADMR spectroscopy

Magnetic-resonance experimental methods such as electron-spin resonance (ESR) and light-induced ESR (LESR) were used before to reveal the CT in polymer-C_{60} mixtures.[52] Using the ESR technique it was shown that there is CT reaction in the ground state of poly(alkylthiophene) PAT-C_{60} composite.[17] Two resonances were found in PAT-C_{60} composites; one at $g=2.002$, which is due to the doping induced polaron in the polymer, and the other at $g=1.999$ associated with C_{60}^- anion.

To study the photoinduced CT process in the PDPA-nBu/C_{60} composite, PADMR measurements were also performed. Figure 12 displays the λ-PADMR spectrum compared to the PA spectrum of PDPA-nBu/7% C_{60} mixture. The PADMR spectrum shows the photoinduced CT signature, namely, a band at 1.15 eV that is due to the C_{60}^- anion. The band associated with C_{60}^- goes together with the S^+ PA band showing the same sign, thus the PADMR spectrum reproduces the PA spectrum. The positive sign of the S^+ and C_{60}^- PADMR bands implies that they are associated with a geminate recombination process.[29,30] This means that a charged soliton is generated as a result of two exciton dissociation onto two dopant C_{60} molecules having spins in an antiparallel configuration following charge separation. This would imply an exciton diffusion on a small distance before the electron transfer. The speed of the CT process, which is estimated to be less than 1 ps,[20] supports the small diffusion length of the exciton, which seems to be important in keeping the spins in antiparallel configuration.

The other features associated with spin-(1/2) resonance in the λ-PADMR spectrum are explained by the distant pair model,[29,53] implying that both neutral soliton and polaron recombination processes are related with the same types of spin pairs. One of the interesting aspects of the λ-PADMR spectrum is the reversed intensity ratio of the neutral soliton band to the polaron band, as compared with that in the PA spectrum. This can be explained assuming a branching process that involves the spin parallel pairs. One part of the parallel spin pairs contributes to processes related to the polaron, while the other part contributes to processes related to the neutral soliton. Another peculiarity of the λ-PADMR spectrum is a huge disproportion between the strength of the high-energy polaron band at 2.4 eV and the low-energy band at 0.3 eV, which are reversed with respect to those found in the PA spectrum. This might be attributed to the EA signal induced by the electric-field modulation of the photoinduced charged species (charged solitons and polarons), which overlaps with the PADMR signal, reducing the signal associated with the high-energy polaron band absorption.[47]

The charge separation in PDPA-nBu/C_{60} can be also observed in the H-PADMR spectrum at 1090 nm (Fig. 13), where the two PADMR resonances that correspond to P^+ and the C_{60}^- anion, respectively, are well resolved.[52] Fitting the H-PADMR spectrum with two Lorentzians we found that

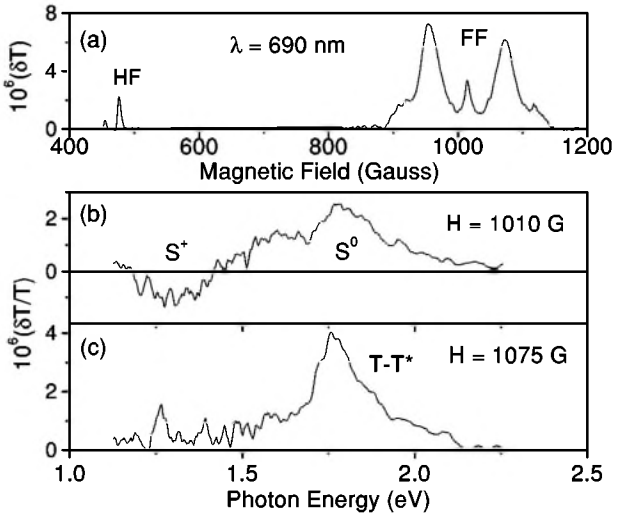

FIG. 14. The PADMR spectra of 7% PDPA-nBu/C_{60}: (a) H scan at 690 nm and (b) λ scan at 1010 G showing the neutral soliton and charged soliton bands, respectively, and (c) λ scan at 1075 G showing the triplet PA band in C_{60}.

the species associated with P^+ has a resonance at $H = 1011$ G with a g factor of 2.12, whereas the C_{60}^- anion has resonance at $H = 1016$ G, with $g = 2.11$.

The two spectral contributions associated with the PA band at 1.7 eV can be resolved in our PADMR measurements [Figs. 14(b,c)]. This PA band has contributions from two different transitions: one transition is attributed to the neutral soliton[5] and the other to the C_{60} triplet.[46,54] The spin-(1/2) reasonance at 1010 G [Fig. 14(b)] corresponds to S^0, whereas the powder pattern shape resonance centered at 1010 G that correlates with a resonance at $H = 475$ G is related to the C_{60} triplet [Fig. 14(c)]. Triplet powder patterns are determined by the anisotropy of the zero-field splitting (ZFS) tensor, whose elements depend on the ZFS E and D parameters.[17] The H-PADMR spectrum with probe wavelength set at 690 nm is displayed in Fig. 14(a) and shows both the full field (FF) and half field (HF) powder patterns of the C_{60} triplet, as well as the doublet resonance associated with the neutral soliton S^0.

The two bands peaking at 975 G and 1075 G, respectively, are associated with the powder pattern related to the $\Delta m = \pm 1$ transitions, while the band peaking at 475 G (HF) is associated with $g = 4$ transitions.[55] The HF powder patern, which formally is ascribed to $\Delta m = \pm 2$, becomes allowed due to the mixture of the Zeeman states as a consequence of the interaction of the spin magnetic dipoles. The three splitted energy levels due to spin related magnetic dipole-dipole interaction depend on the ZFS parameters, E and D, which can be estimated from the FF triplet powder pattern. The values obtained for the ZFS parameters from FF resonances are $E = 0$ eV and $D = 1.42 \times 10^{-6}$ eV (0.0115 cm^{-1}), which are close to the values obtained for the C_{60} triplet (0.0117 cm^{-1}).[54,55]

Figure 14(b) shows the λ-PADMR spectrum between 1–2.25 eV for the doublet resonances at 1010 G: the spectrum shows neutral soliton, charged soliton, and C_{60}^- related resonances. The feature associated to C_{60}^- is not clearly resolved in this measurement due to a lower signal-to-noise ratio. The λ-PADMR spectrum for the resonance at 1075 G shown in Fig. 14(c) exhibits only one band, which is the evidence for the C_{60} triplet.

IV. CONCLUSIONS

In this work we investigated the photophysical properties of PDPA-nBu. We found that PDPA-nBu has strong PL with quantum efficiency of about 60%. The PL excitation dependence and the polarized PL measurements show that the PL emission originates from the radiative recombination of intrachain excitons. The strong PL emission in PDPA-nBu, which is a degenerate ground state, is explained by the order of the lowest-lying exciton state: $1B_u$ lies lower than $2A_g$ due to a small on-site Coulomb interaction in this polymer. This energetics is opposite to that in trans-$(CH)_x$. The relatively small on-site electron-electron interaction in PDPA-nBu is due to the screening effect of the polymer bulky side groups, which also leads to a transversal delocalization and a confinement of the exciton along the chain. The effective on-site electron-electron interaction can be thus written as $U_{eff} = U - W_t$, where W_t originates from the transversal electron delocalization.[7,8] In PDPA-nBu, U_{eff} is ≈ 0.6 eV,[5] which is much smaller compared with $U_{eff} = 0.9$ eV obtained in trans-$(CH)_x$.[56]

The PDPA-nBu absorption bands were identified, correlating the experimental data and theoretical model.[7] The three absorption bands were assigned as follows: the lowest-energy band accompanied by the vibronic side bands was ascribed to intrachain exciton; the second band peaking around 4.2 eV is due to a CT transition between the chain and phenyl side groups; and the high-energy band is due to the phenyl ring absorption.

The PA spectrum in PDPA-nBu toluene solution indicates that long-lived polarons are photogenerated, although polarons were considered before to be unstable in DGS polymers. The PA spectrum of the pristine PDPA-nBu film, on the contrary, displays a strong PA band at 1.7 eV assigned to neutral solitons and two small bands at 0.3 eV and 2.3 eV, respectively, which were assigned to polarons. The polarons may be created in polymer solution by CT between the polymer and solvent or by CT between two adjacent conjugated segments on the same chain or neighboring chains. The lack of soliton PA in the PDPA-nBu solution may be due to excess confinement of the photoexcitations in the short conjugated segments. The confinement does not allow a lattice distortion with change in phase that is related to soliton-antisoliton pairs to occur due to the shortening of the conjugation length. The observed blueshift of the absorption spectrum of PDPA-nBu in solution compared to the absorption in films is in agreement with the shortening of the chain conjugation length.

Using PA and PADMR spectroscopies it was shown that in PDPA-nBu/C_{60} blends CT reaction takes place in the excited states. No features associated with CT were seen in the linear absorption spectrum of the mixture. The PA spectrum of the blend shows the signature of the photoinduced CT

reaction, namely, a PA band peaking at 1.15 eV due to the photogenerated C_{60}^-. It also indicates the existence of long-lived polaron and soliton excitations on the polymer chains. Close to the high-energy polaron band at 2.4 eV, photobleaching was found and was attributed to photoinduced EA of the C_{60} due to the electric field associated with the photogenerated charged species. The qualitative change of the PA spectrum in the high-energy polaron region depends on the inhomogeneties in the sample due to the C_{60} segregation in the blend. It was shown that charged solitons are also generated on the polymer chains via the photoinduced CT process as a result of dissociation of two excitons into two adjacent C_{60} molecules, resulting in a pair of charged solitons in the polymer chain and two C_{60}^- ions. Two different photogeneration channels were found for polarons in PDPA-C_{60}: one via polymer excitation and the other via C_{60} excitation. In the polymer excitation channel the exciton dissociates into a C_{60} molecule, whereas in the C_{60} excitation channel a hole transfer takes place when the C_{60} molecule is photoexcited.

Evidence for photoinduced CT in PDPA-nBu/C_{60} was also found in PADMR measurements. λ-PADMR spectra showed a band at 1.15 eV ascribed to C_{60}^- for magnetic field corresponding to spin-(1/2) resonance. The H-PADRM scan at 1090 nm shows two resonances associated with polarons and C_{60}^-, respectively. Fitting the resonance band at 1090 nm with two Lorentzians, we obtain the g factors of the two species; one at $g=2.12$ for polarons and the other at $g=2.11$ for C_{60}^-.

ACKNOWLEDGMENTS

The work at the University of Utah was supported in part by DOE Grant No. ER 45490 and NSF Grant No. DMR 02-02790.

[1] B. S. Hudson, B. E. Kohler, and K. Schulten, in *Excitated States*, edited by E. C. Lim (Academic, New York, 1982).
[2] S.N. Dixit, D. Guo, and S. Mazumdar, Phys. Rev. B **43**, 6781 (1991).
[3] Z.G. Soos, S.E. Etemand, D.S. Galvao, and S. Ramasesha, Chem. Phys. Lett. **194**, 341 (1992).
[4] K. Tada *et al.*, SPIE Int. Soc. Opt. Eng., Proc. **3145**, 171 (1998).
[5] I. Gontia, S.V. Frolov, M. Liess, E. Ehrenfreund, K. Tada, H. Kajii, R. Hydayat, A. Fujii, K. Yoshino, M. Teraguchi, and T. Masuda, Phys. Rev. Lett. **82**, 4058 (1999).
[6] A.J. Heeger, K. Kievelson, J.S. Schrieffer, and W.P. Su, Rev. Mod. Phys. **60**, 781 (1988).
[7] H. Ghosh, A. Shukla, and S. Mazumdar, Phys. Rev. B **62**, 12 763 (2000).
[8] A. Shukla and S. Mazumdar, Phys. Rev. Lett. **83**, 3944 (1999); A. Shukla, H. Ghosh, and S. Mazumdar, Synth. Met. **116**, 87 (2001).
[9] N.T. Harrison, G.R. Hayes, R.T. Phillips, and R. Friend, Phys. Rev. Lett., **77**, 1881 (1996).
[10] R. Hidayat, S. Tatsuhara, D.W. Kim, M. Ozaki, K. Yoshino, M. Taraguchi, and T. Masuda, Phys. Rev. B **61**, 10 167 (2000).
[11] S.V. Frolov, M. Shkunov, Z.V. Vardeny, K. Tada, R. Hydayat, M. Hirohata, M. Teraguchi, T. Masuda, and K. Yoshino, Jpn. J. Appl. Phys., Part 2 **36**, L1268 (1997).
[12] K. Tada, R. Hidayat, M. Hirohata, M. Teraguchi, T. Masuda, and K. Yoshino, Jpn. J. Appl. Phys., Part 2 **35,**, L1138 (1996).
[13] S. Morita, A.A. Zakhidov, and K. Yhoshino, Solid State Commun. **82**, 249 (1992).
[14] N.S. Sariciftci, L. Smilowitz, A.J. Heeger, and F. Wudl, Science **258**, 1474 (1992).
[15] K. Yoshino, X.H. Yin, S. Morita, and A.A. Zakhidov, Jpn. J. Appl. Phys., Part 2 **32**, L140 (1993).
[16] S. Luzzati *et al.*, Mol. Cryst. Liq. Cryst. Sci. Technol., Sect. A **256**, 927 (1994).
[17] K. Lee , R.A. Janssen, N.S. Sariciftci, and A.J. Heeger, Phys. Rev. B **49**, 5781 (1994).
[18] S.B. Lee, A.A. Zakhidov, I.I. Khairullin, V.Yu. Sakalov, P.K. Khabibullaev, K. Tada, K. Yoshimoto, and K. Yoshino, Synth. Met. **77**, 155 (1996).
[19] J.J.M. Halls, K. Pichler, R.H. Friend, S.C. Moratti and A.B. Holmes, Appl. Phys. Lett. **68**, 22 (1996).
[20] K. Karabel, C.H. Lee, D. McBranch, D. Moses, N.S. Sariciftci, and A.J. Heeger, Chem. Phys. Lett., **213**, 389 (1993).
[21] K. Hasharoni, M. Keshavarz-K, A. Sastre, R. Gonzalez, C. Bellavia-Lund, Y. Greenwald, T. Swager, F. Wudl, and A.J. Heeger, J. Chem. Phys. **107**, 2308 (1997).
[22] K. Harigaya, Phys. Rev. B **45**, 13 676 (1992).
[23] N. Sariciftci, B. Karabel, C.H. Lee, K. Pakbaz, D.J. Sandman, and A.J. Heeger, Phys. Rev. B **50**, 12 044 (1994).
[24] M.J. Rice and Yu.N. Garstein, Phys. Rev. B **53**, 10 764 (1996).
[25] T. Masuda, T. Hamano, K. Tsuchihara, and T. Higashimura, Macromolecules **23**, 1374 (1990).
[26] H. Shirakawa, T. Masuda, and K. Takeda, in *The Chemistry of Triple-bounded Functional Groups*, edited by Saul Patai (Wiley, New York, 1994), Chap. 17, p. 945.
[27] I. Gontia, S.V. Frolov, M. Liess, Z.V. Vardeny, E. Ehrenfreund, K. Tada, H. Kajii, R. Hydayat, A. Fujii, K. Yoshino, M. Teraguchi, and T. Masuda, Synth. Met. **116**, 91 (2001).
[28] D. Comoretto, G. Dellepiane, F. Marabelli, P. Tognini, A. Stella, J. Cornil, D.A. dos Santos, J.L. Bredas, and D. Moses, Synth. Met. **116**, 107 (2001).
[29] Z. V. Vardeny and X. Wei, in *Handbook of Conducting Polymers*, 2nd ed., edited by T. Skotheim, R. Elsenbaumer, and J. R. Reynolds (Dekker, New York, 1997), p. 639.
[30] I. I. Gontia, Ph.D. thesis, University of Utah, 2002 (unpublished).
[31] G.B. Blanchet, C.R. Fincher, and A.J. Heeger, Phys. Rev. Lett. **50**, 1938 (1983).
[32] X. Wei, B.C. Hess, Z.V. Vardeny, and F. Wudl, Phys. Rev. Lett. **68**, 666 (1992).
[33] X. Wei, Ph.D. thesis, University of Utah, 1992, and the references therein (unpublished).
[34] A. Fujii, R. Hidayat, T. Sonoda, T. Fujisawa, M. Ozaki, Z.V. Vardeny, M. Teraguchi, T. Masuda, and K. Yoshino, Synth. Met. **116**, 95 (2001).

[35] M. Wohlgennant, W. Graupner, G. Leising, and Z.V. Vardeny, Phys. Rev. B **60**, 5321 (1999).
[36] O. Korovyanko, I. I. Gontia, and Z. V. Vardeny (unpublished).
[37] P. Tavan and K. Schulten, Phys. Rev. B **36**, 4337 (1987).
[38] G.W. Hayden and E.J. Mele, Phys. Rev. B **34**, 5484 (1986).
[39] W.P. Su, Phys. Rev. B **34**, 2988 (1986).
[40] Z. Vardeny, J. Orenstein, and G.L. Baker, Phys. Rev. Lett. **50**, 2032 (1983).
[41] C. Botta, S. Luzzati, R. Tubino, D.D.C. Bradeley, and R.M. Friend, Phys. Rev. B **48**, 14 809 (1993).
[42] T.L. Gustafson, E.M. Kyllo, T.L. Frost, R.G. Sun, H. Lim, D.K. Wang, A.J. Epstein, C. Lefumeux, G. Buntinx, and O. Poisat, Synth. Met. **116**, 31 (2001).
[43] S.L. Ren, Y. Wang, A.M. Rao, E. McRae, J.M. Holden, T. Hager, KaiAn Wang, Wen-Tse Lee, H.F. Ni, J. Selegue, and P.C. Eklund, Appl. Phys. Lett. **59**, 2678 (1991).
[44] B. Horovitz, Solid State Commun. **41**, 729 (1982).
[45] T. Kato, T. Kodama, T. Shida, T. Nakagawa, Y. Matsui, S. Suzuki, H. Shiromaru, K. Yamauchi, and Y. Achiba, Chem. Phys. Lett. **180**, 446 (1991).
[46] M. Lee, M. Lee, O. Song, J. Seo, and D. Kim, Chem. Phys. Lett. **196**, 325 (1992).
[47] D. Dick, X. Wei, S. Jeglinski, R.E. Benner, Z.V. Vardeny, D. Moses, S.I. Srdanov, and F. Wudl, Phys. Rev. Lett. **73**, 2760 (1994).
[48] S. Jeglinski, Z.V. Vardeny, D. Moses, and F. Wudl, Synth. Met. **50**, 557 (1992).
[49] M. Wohlgennant, W. Graupner, G. Leising, and Z.V. Vardeny, Phys. Rev. Lett. **82**, 3344 (1999).
[50] M. Wohlgennant, W. Graupner, F.P. Wentzl, S. Tasch, E.J.W. List, G. Leising, M. Graupner, A. Hermetter, U. Rohr, P. Schlihting, Y. Geerts, U. Scherf, and K. Mullen, Chem. Phys. **227**, 99 (1998).
[51] W. Graupner, G. Leditzky, and G. Leising, Phys. Rev. B **54**, 7610 (1996).
[52] L. Smilowitz, N.S. Sariciftci, R. Wu, C. Gettinger, A.J. Heeger, and F. Wudl, Phys. Rev. B **47**, 13 835 (1993).
[53] M. Wohlgennant, K. Tandon, S. Mazumdar, R. Ramasesha, and Z.V. Vardeny, Nature (London) **409**, 494 (2001).
[54] X. Wei and Z.V. Vardeny, Phys. Rev. B **52**, R2317 (1995).
[55] P. Lane, L.S. Swanson, Q-X. Ni, and J. Shinar, Phys. Rev. Lett. **68**, 887 (1992).
[56] W.P. Su, Phys. Rev. Lett. **74**, 1167 (1995); J. Orenstein, in *Handbook of Conducting Polymers*, edited by T. Skotheim (Dekker, New York, 1986), Vol. 2, Chap. 36, p. 1297.